

Supporting information for

## **Adhesive Sponge Based on Supramolecular Dimers Interactions as Scaffolds for Neural Stem Cells**

*Luanda LINS<sup>a\*</sup>, Florence WIANNY<sup>b</sup>, Colette DEHAY<sup>b</sup> Jacques Jestin<sup>c</sup>, Watson Loh<sup>a</sup>.*

**Supporting data:** Number of pages: 13

Number of Figures: 9

Number of Tables: 2

### **Table of contents:**

Experimental Section: Synthesis of Agarose-Br.

Experimental Section: Synthesis of Agarose-N<sub>3</sub>.

Experimental Section: Synthesis of Agarose-NH<sub>2</sub>.

Experimental Section: Synthesis of Agarose-UPy.

Results and Discussion Section - Figure S1: <sup>1</sup>H NMR spectrum of UPy-Synthon synthesis.

Results and Discussion Section - Figure S2: Scheme of Agarose modification.

Results and Discussion Section - Figure S3: AGA-NH<sub>2</sub> synthesis description and FTIR characterization.

Results and Discussion Section - Table S1: Characteristic FTIR bands of agarose.

Results and Discussion Section - Figure S4: <sup>13</sup>C NMR repeating units of agarose and <sup>13</sup>C NMR table with assignment.

Results and Discussion Section - Table S2: TGA analysis of UPy-NCO, AGA-NH<sub>2</sub>, and AGA-UPy.

Results and Discussion Section - Figure S5: Stress-strain curve of sponges.

Results and Discussion Section - Figure S6: Surface roughness of the sponges-like scaffold.

Results and Discussion Section - Figure S7: Cell proliferation.

Results and Discussion Section - Figure S8: Cell distribution into sponges-like scaffold.

Results and Discussion Section - Figure S9: Integration of NSCs in sponge-like scaffolds.

References.

## Experimental Section

### General procedure for the synthesis of Agarose-Br

The bromination of agarose was carried out following the literature <sup>17</sup>. A pristine agarose (5 g) and LiCl (6.47 g, 10 eq. vs. galactose unit) were added into dry DMF (175 mL) and the mixture was stirred at 80 °C for 24 h under an argon atmosphere to form a transparent solution. To the solution, a triphenylphosphine (2.5 eq. vs. galactose unit, 50.5 g) dry DMF solution was added and the resulting mixture was stirred at *r.t.* for 3 h.

After cooling the mixture to 0 °C, a CBr<sub>4</sub> (1 eq. vs. galactose unit, 12.5 g) dry DMF solution (120 mL) was gradually added and the resulting mixture was stirred at 40 °C. The mixture was poured into a 1/1 MeOH–water solution (2 L) to form a precipitate. The precipitate was collected using a centrifuge, washed with MeOH, and dried in vacuum to afford AGA-Br as a pale brown solid.

### General procedure for the synthesis of Agarose-N<sub>3</sub>

AGA-Br (3–5 g) was added into DMSO (350 mL) and the mixture was stirred to forming a transparent solution. Then, NaN<sub>3</sub> (10 eq. vs. glucose unit) was added at 80 °C and the mixture was stirred for 48 h. After cooling to *r.t.*, the mixture was spilled into water (600 mL) forming a precipitate. The precipitate was compiled using a centrifuge, washed with water, and freeze-dried to afford AGA-N<sub>3</sub> as a colorless solid (2.79 g).

### General procedure for synthesis of Agarose-NH<sub>2</sub>

AGA-N<sub>3</sub> (2 g) was added into DMSO (300 mL) and the mixture was stirred for 20 min at 80 °C to suspend a precipitate. To the suspension, 4.33 g of NaBH<sub>4</sub> (30 eq. vs. galactose unit) was added and the mixture was stirred for 48 h at 80 °C. Subsequently, MeOH (60 mL) was added into the reaction mixture yielding a precipitate. The product was collected and purified by dialysis (milli-q water) for 1 week, followed by freeze-drying to afford AGA-NH<sub>2</sub> as a colorless solid.

### General procedure for the synthesis of Agarose-UPy

Compound AGA-NH<sub>2</sub> (9.2 mmol, 18.4 g) was poured into dry CHCl<sub>3</sub> (300 mL). UPy-synthon (21.8 mmol, 6.4 g) was added and stirred under argon for 4 h at *r.t.*. Unreacted UPy-NCO was removed by reaction with an amine-resin and stirred for 2 h at *r.t.* The mixture was filtered over Hyflo Super Cell and 15 mL MeOH was added. The product was precipitated in 2.5 L ethyl ether, filtered, dried under vacuum to afford AGA-UPy as a white powder (93 %, yield = 22.25 g).

## Results and Supporting Discussion

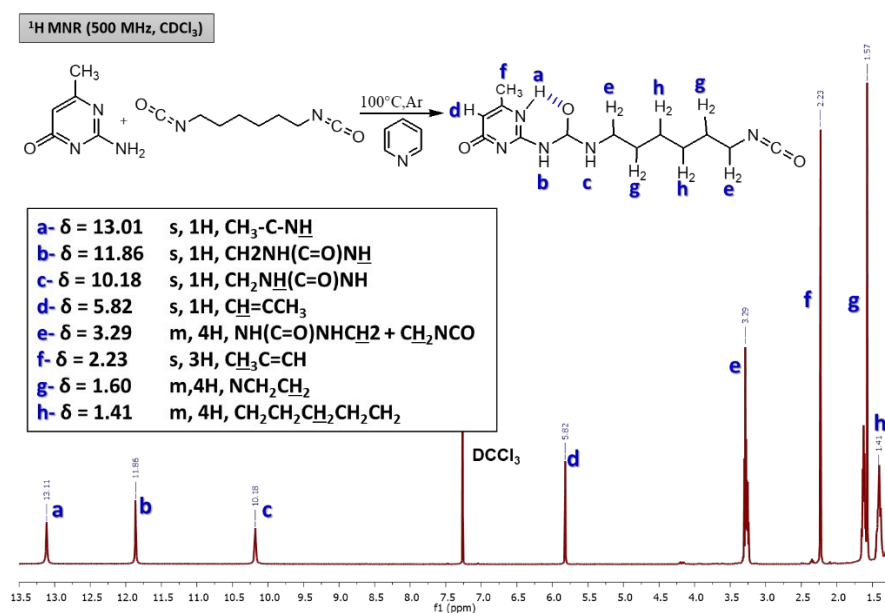


**Figure S1.** Schematic pathway of 2-(6-Isocyanatohexylaminocarbonylamino)-6-methyl-4(1H)-pyrimidinone and <sup>1</sup>H NMR spectrum of UPy-Synthon in CDCl<sub>3</sub>. The presence of peaks at  $\delta = 10.18$ ,  $11.85$ , and  $13.01$  ppm reveals hydrogen-bonded amines and thus suggest UPy in good agreement with the results of Beijer *et al*<sup>1-4</sup>.

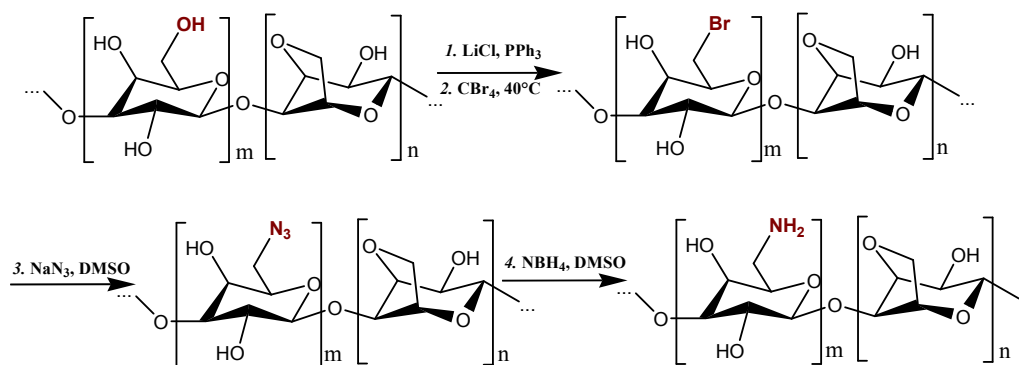


**Figure S2.** Chemo-selective coupling to produce Agarose-Synthons.

**Agarose Bromination - Pre-“Click” Functionalization:** Native linear agarose (AGAR) was first converted into 6-bromo-6-deoxy-agarose (AGAR-Br) by Pre-“Click” Functionalization according to the literature <sup>5</sup>. The Appel reaction is somewhat similar to the Mitsunobu Reaction, where the combination of a phosphine, a diazo compound as a coupling reagent, and a nucleophile are used to invert the stereochemistry of an alcohol or displace it. This reaction of triphenylphosphine (CBr<sub>4</sub>) with alcohols is a ready method to convert an alcohol to the corresponding alkyl halide under mild conditions (Figure S2). The reaction proceeds by activation of the triphenylphosphine by reaction with the tetrahalomethane, followed by attack of the alcohol oxygen at phosphorus to generate an oxyphosphonium intermediate. The oxygen is then transformed into a leaving group, and an SN<sub>2</sub> displacement by halide takes place, proceeding with inversion of configuration if the carbon is asymmetric <sup>6</sup>.

The exclusive conversion of primary hydroxy-groups into bromide-groups was confirmed by FTIR and XPS of the product.

**“Click” Functionalization: Agarose Azidation -Reduction reaction:** In this study, the click chemistry based on azides addition was chosen to functionalize agarose with amines groups, denote AGA-NH<sub>2</sub>. The FTIR spectral bands of agarose and agarose derivatives were compared with those reported earlier in the literature for validation purpose (Figure S2) <sup>7-9</sup>. The principal bands for agarose were observed at 3395 cm<sup>-1</sup> (OH, axial deformation), 2904 cm<sup>-1</sup> (CH, axial deformation), 1158 and 1071 cm<sup>-1</sup> (C-O, axial deformation), 930 cm<sup>-1</sup> (characteristic of 3,6-anhydrogalactose) and 891 cm<sup>-1</sup> (attributed to CH angular deformation of β anomeric carbon). The band at 1741 cm<sup>-1</sup> not present in neat agarose spectrum was attributed to the C=O group and directly connected to the chemical modification.

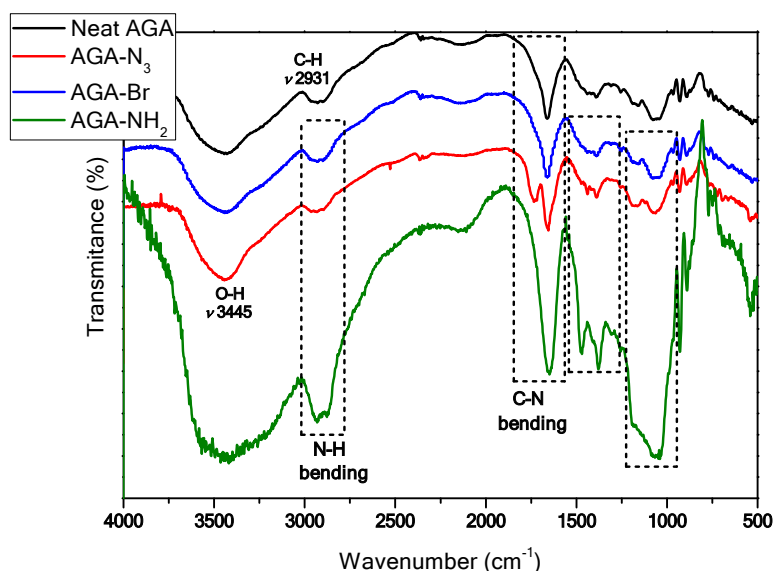


**Figure S3.** FTIR spectra of unmodified agarose and modified agarose AGA-Br, AGA-N<sub>3</sub>, and AGA-NH<sub>2</sub>.

Table 1 details the bands characteristic of agarose. A moderately intense band is found in the region 1730-1684  $\text{cm}^{-1}$  which may be due to the C-N stretching vibrations in azide-agarose. The anomalous splitting of the  $\text{N}_3$  stretching bands have been explained in terms of Fermi interaction with combination tones involving the  $\text{N}_3\text{CH}_2\text{CH-O-}$  <sup>10</sup>.

**Table S1.** Characteristic bands of the IR spectra of agarose.

| $\nu_{\text{max}}$ ( $\text{cm}^{-1}$ )* | Agarose vibration                                 |
|--|---|
| 3434br                                   | (-OH, stretching vibration)                       |
| 2924w                                    | -CH <sub>2</sub> , stretching vibration           |
| 1630w                                    | H-O-H, stretching vibration of bound water        |
| 1461w                                    | C-C, bending vibration                            |
| 1378w                                    | methylene group                                   |
| 1154,<br>1077br                          | C-O-C, stretching vibration of glycosidic linkage |
| 930m                                     | 3,6-anhydro galactose                             |

\* band intensities: br= broad; m= medium; w= weak.

|                              |                                  |                          |                      |                                 |                        |                                   |
|------------------------------|----------------------------------|--------------------------|----------------------|---------------------------------|------------------------|-----------------------------------|
|                              |                                  |                          |                      |                                 |                        |                                   |
| <b>G1:</b> 101.22 ppm        | <b>A1:</b> 99.76 ppm             | <b>G3, A3:</b> 80.14 ppm | <b>1:</b> 18.50 ppm  | <b>2:</b> 149.82 ppm            | <b>3:</b> 107.80 ppm   | <b>4:</b> 174.43 ppm              |
| <b>A4, G5, A5:</b> 76.00 ppm | <b>G2, G4, A2, A6:</b> 70.03 ppm | <b>G6:</b> 62.60 ppm     | <b>5:</b> 156.89 ppm | <b>9 + 10:</b> 30.69, 29.35 ppm | <b>8+11:</b> 39.82 ppm | <b>7+12:</b> 44.57 ppm, 43.11 ppm |

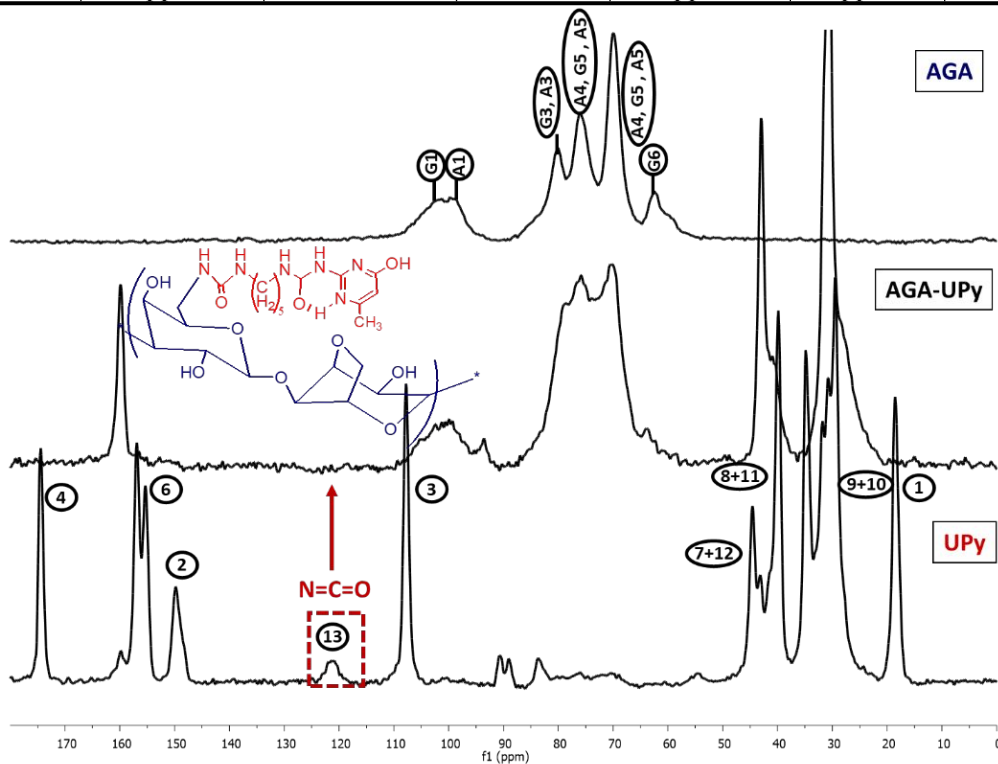


**Figure S4.** Representation of the chemical structure of disaccharide repeating units of agarose (G: 1,3-b-D-galactose and A: 1,4-a-L-3,6-anhydrogalactose) and UPy. Table with assignment on unmodified agarose, UPy and synthesized AGA-UPy<sup>11-13</sup>. <sup>13</sup>C CPMAS spectra of the modified agarose compared with unmodified agarose and UPy.

**Table S2.** Thermal degradation UPy precursor, amine-agarose, and Agarose-UPy (N<sub>2</sub> 10°C/min)

| UPy                 | <u>T1</u>      | <u>T2</u>      | <u>T3</u>        | <u>T4</u> | <u>Total deg</u> |
|---------------------|----------------|----------------|------------------|-----------|------------------|
| Degradation         | 13%            | 59%            | 13,50%           | 8%        | 94%              |
| Tonset (°C)         | 170,5          | 268            | 467              | 590       |                  |
| Tmax (°C)           | 175,6          | 293            | 479              | 642       |                  |
| AGA-NH <sub>2</sub> | <u>T1</u>      | <u>T2</u>      | <u>Total deg</u> |           |                  |
| Degradation         | 8%             | 64%            | 74%              |           |                  |
| Tempin (°C)         | 47,9           | 260            |                  |           |                  |
| Tmax (°C)           | 57             | 272            |                  |           |                  |
| AGA-UPy             | <u>T1 (°C)</u> | <u>T2 (°C)</u> | <u>Total deg</u> |           |                  |
| Degradation         | 8.7%           | 85%            | 93%              |           |                  |
| T onset (°C)        | 254            | 607            |                  |           |                  |
| Tmax (°C)           | 287            | 676            |                  |           |                  |

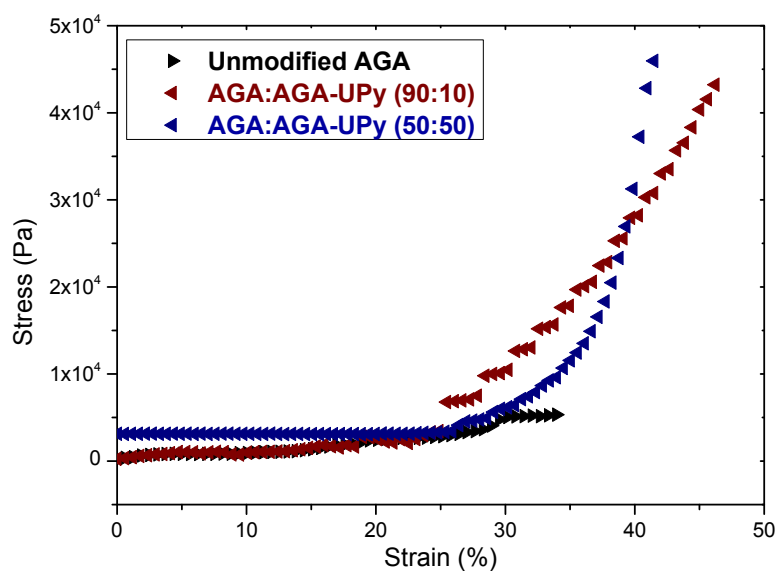


**Figure S5.** Stress-strain curve of unmodified AGA, AGA:AGA-UPy (90:10), and AGA:AGA-UPy (50:50) sponges under unconfined compression (ramp 50% strain at speed of 1 mm/min) (n = 3).

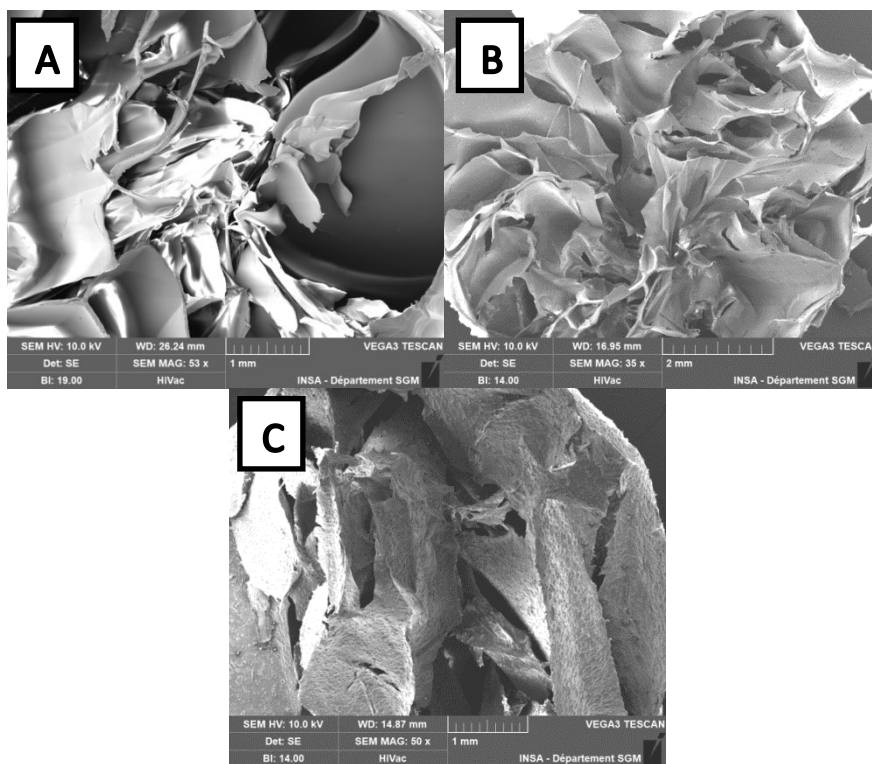


**Figure S6.** SEM micrographs showing the surface roughness of the sponges-like scaffold (A) unmodified AGA, (B) AGA:AGA-UPy (90:10), and (C) AGA:AGA-UPy (50:50).

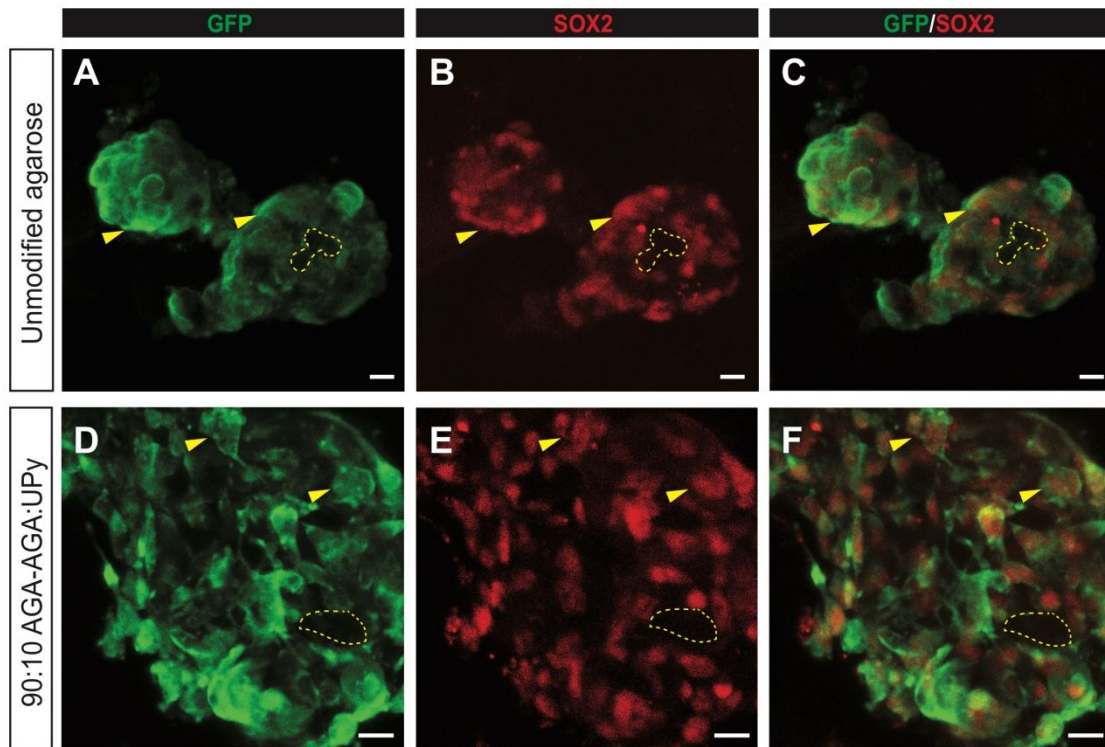


**Figure S7.** Characterization of NSCs following culture in unmodified agarose and AGA-AGA:UPy scaffolds. Confocal images of NSCs stained for GFP (Green) (**A,D**) and SOX2 (Red) (**B,E**). (**C,D**), Merge images of GFP and SOX2 stainings. A majority of GFP-positive cells express SOX2 (as indicated by yellow arrows). GFP-negative regions are negative for SOX2 (marked by yellow dotted lines). Scale bars: 10 $\mu$ m.

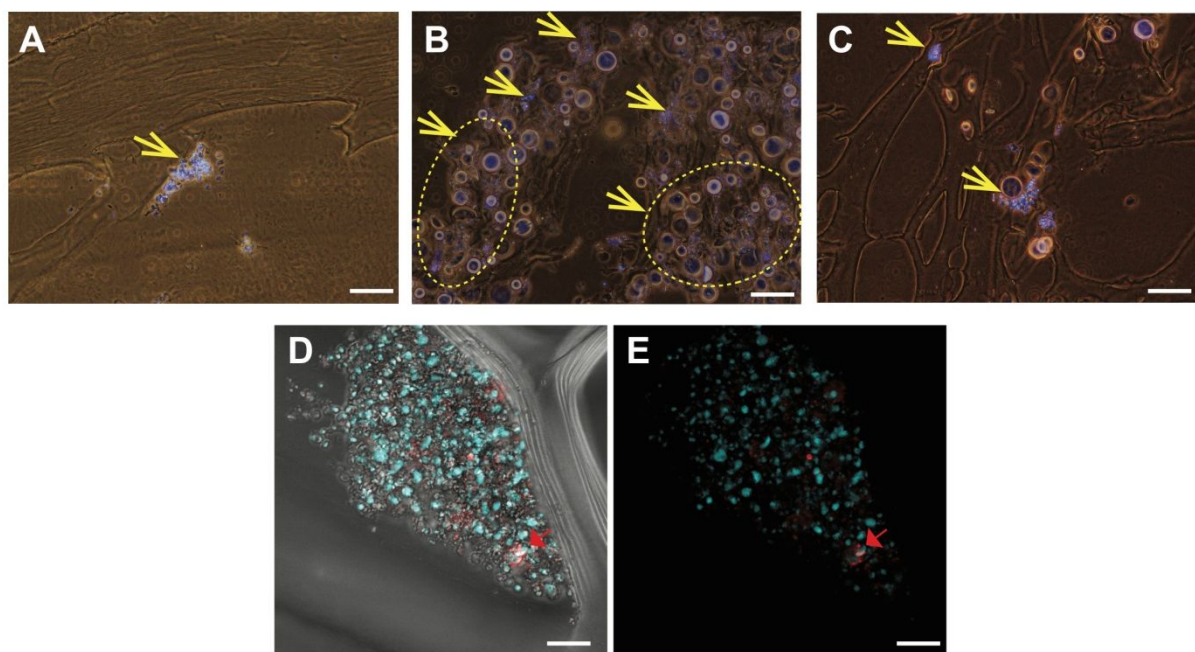


**Figure S8.** (A-C), Sponges-like scaffolds following cell distribution on (A) unmodified AGA, (B) AGA-AGA:UPy 50:50, and (C) AGA-AGA:UPy 90:10. (A-C) Merged images of nuclei stained with DAPI (cyan) and phase contrast images (grey). Yellow arrows indicate the cell position stained with DAPI (blue). Scale Bars, 100  $\mu\text{m}$ . (D, E) High cell-death rate of NSCs in unmodified AGA; (D) Merge images of nuclei stained with DAPI (cyan), F-Actin stained with Phalloidin (red), and phase contrast images (grey). (E) shows high cell death, as shown high DNA fragmentation and rare F-Actin staining (red arrow). Merge images of nuclei stained with DAPI (cyan) and F-Actin stained with Phalloidin (red). Scale Bars, 20  $\mu\text{m}$ .

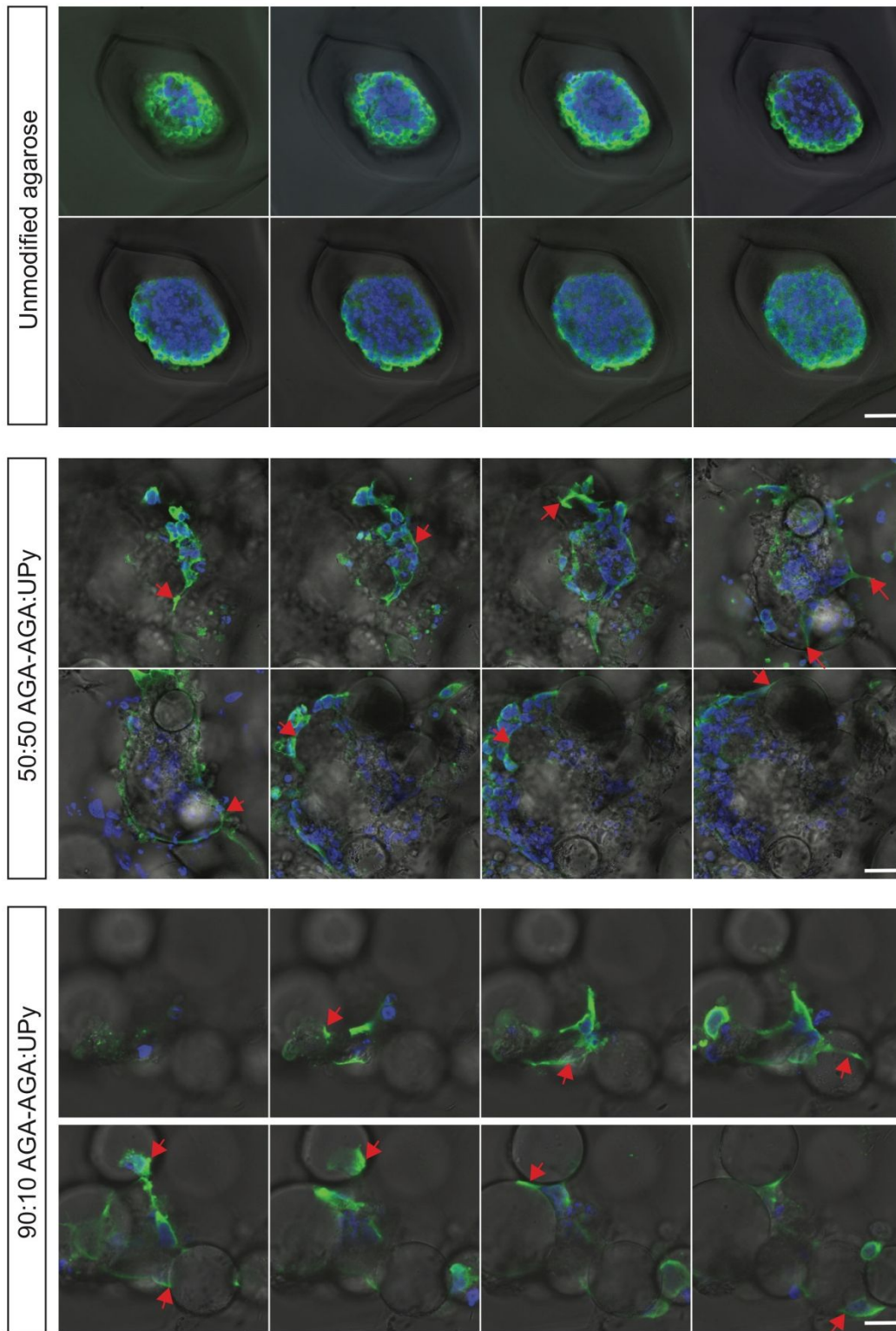


**Figure S9.** Integration of NSCs in sponge-like scaffolds. Z-stack confocal microscopy images taken at 3  $\mu\text{m}$  intervals through the scaffolds. Cell-scaffold contacts are visible at different levels in the thickness of AGA-AGA:UPy sponges (Red arrows). No contacts are visible between cells and unmodified agarose scaffold. Merge images of nuclei stained with DAPI (blue), GFP (green), and phase contrast images (grey). Scale bars, 10 $\mu\text{m}$ .

## References

1. Jangizehi, A.; Ghaffarian, S. R.; Kowsari, E.; Nasser, R., Supramolecular Polymer Based on Poly (Ethylene-co-Vinyl Alcohol)-g-Ureidopyrimidinone: Self-Assembly and Thermo-Reversibility. *J Macromol Sci B* **2014**, *53*, 848-860.
2. B., F. B. J.; P., S. R.; M., V. R.; J., v. d. R. J. A.; W., M. E., Supramolecular Polymer Materials: Chain Extension of Telechelic Polymers Using a Reactive Hydrogen-Bonding Synthon. *Adv. Mater.* **2000**, *12*, 874-878.
3. Dankers, P. Y. W.; van Leeuwen, E. N. M.; van Gemert, G. M. L.; Spiering, A. J. H.; Harmsen, M. C.; Brouwer, L. A.; Janssen, H. M.; Bosman, A. W.; van Luyn, M. J. A.; Meijer, E. W., Chemical and biological properties of supramolecular polymer systems based on oligocaprolactones. *Biomaterials* **2006**, *27*, 5490-5501.
4. Beijer, F. H.; Sijbesma, R. P.; Kooijman, H.; Spek, A. L.; Meijer, E. W., Strong Dimerization of Ureidopyrimidones via Quadruple Hydrogen Bonding. *J. Am. Chem. Soc.* **1998**, *120*, 6761-6769.
5. Tamaru, S.-i.; Tokunaga, D.; Hori, K.; Matsuda, S.; Shinkai, S., Giant amino acids designed on the polysaccharide scaffold and their protein-like structural interconversion. *Org. Biomol. Chem.* **2014**, *12*, 815-822.
6. Wang, Z., Appel Reaction. In *Comprehensive Organic Name Reactions and Reagents*. In *Comprehensive Organic Name Reactions and Reagents*, 2010.
7. Chudasama, N. A.; Siddhanta, A. K., Facile synthesis of nano-sized agarose based amino acid—Its pH-dependent protein-like behavior and interactions with bovine serum albumin. *Carbohydr. Res.* **2015**, *417*, 57-65.
8. Chudasama, N. A.; Prasad, K.; Siddhanta, A. K., Agarose functionalization: Synthesis of PEG-agarose amino acid nano-conjugate – its structural ramifications and interactions with BSA in a varying pH regime. *Carbohydr. Polym.* **2016**, *151*, 735-742.
9. Mehta, G. K.; Kondaveeti, S.; Siddhanta, A. K., Facile synthesis of agarose-l-phenylalanine ester hydrogels. *Polym. Chem.* **2011**, *2*, 2334-2340.
10. Lieber, E.; Rao, C. N. R.; Thomas, A. E.; Oftedahl, E.; Minnis, R.; Nambury, C. V. N., Infrared spectra of acid azides, carbamyl azides and other azido derivatives: Anomalous splittings of the N3 stretching bands. *Spectrochim. Acta* **1963**, *19*, 1135-1144.
11. Meena, R.; Siddhanta, A. K.; Prasad, K.; Ramavat, B. K.; Eswaran, K.; Thirupathi, S.; Ganesan, M.; Mantri, V. A.; Rao, P. V. S., Preparation, characterization and benchmarking of agarose from *Gracilaria dura* of Indian waters. *Carbohydr. Polym.* **2007**, *69*, 179-188.
12. Wang, Y.; Zhang, X.; Han, N.; Wu, Y.; Wei, D., Oriented covalent immobilization of recombinant protein A on the glutaraldehyde activated agarose support. *Int. J. Biol. Macromol.* **2018**, *120*, 100-108.
13. Folmer, B. J. B.; Sijbesma, R. P.; Versteegen, R. M.; van der Rijt, J. A. J.; Meijer, E. W., Supramolecular Polymer Materials: Chain Extension of Telechelic Polymers Using a Reactive Hydrogen-Bonding Synthon. *Adv. Mater.* **2000**, *12*, 874-878.